3D Characterization and Time-Lapse Imaging of the Desiccation Treatability Test at the Hanford BC-Cribs and Trenches Site using High Performance Computing applied to Electrical Resistivity Imaging – 12271

Tim Johnson, Jason Greenwood, Chris Strickland, Mike Truex and Vicky Freedman
Pacific Northwest National Laboratory

Glen Chronister
CH2M Hill Plateau Remediation Company

Dale Rucker
HydroGeophysics, Inc.

ABSTRACT

Contaminated vadose zone materials are a potential source of long-term groundwater contamination at many sites across the Department of Energy (DOE) complex. Deep vadose zone contamination presents a particularly challenging remedial problem due to the difficultly of locating contaminants and the expense of access and *ex situ* treatment. *In situ* remediation techniques, whereby remedial amendments must be delivered to contaminated soils, have been identified as a potential alternative. However, amendment delivery is typically uncertain and post delivery remedial performance is often not well understood due to limited information available from sparsely spaced boreholes.

Recent advancements in electrical resistivity tomography (ERT) are being used to address these challenges at the Hanford site by providing remote, three-dimensional images of contaminant distribution and four-dimensional (three spatial dimensions plus the time dimension) images of *in-situ* vadose zone remediation processes. These capabilities were recently demonstrated with a large scale surface characterization effort and during a smaller scale desiccation treatability test at the Hanford BC-Cribs area. The results of these efforts demonstrate the utility of leveraging high-performance computing resources to process ERT data for 3D reconnaissance mapping of subsurface contaminants and for detailed 3D monitoring of vadose zone remediation efforts.

INTRODUCTION

Vadose zone materials are a potential source of groundwater contamination at many sites across the Department of Energy (DOE) complex. Deep vadose zone contaminants present a particularly challenging remedial problem due to the difficulty and expense of access and *ex situ* treatment. *In situ* remediation techniques have been identified as a potential alternative. Most *in situ* methods require that amendments be delivered to contaminated areas. However, *a priori* prediction of amendment delivery is typically uncertain due the variability in parameters that

govern amendment flow and transport. In addition, post delivery remedial performance is often not well understood due to limited information available from sparsely spaced boreholes. For the same reasons, critical capabilities to monitor post-delivery contaminant mobility are limited with borehole sampling alone. Hence, methods are needed that can 1) characterize contaminant distributions between boreholes and away from sensor locations 2) reduce uncertainty in estimating the 3D distribution of parameters that govern flow and transport, 3) monitor and validate amendment delivery in 3D, and 4) monitor post-delivery remedial performance in 3D, including contaminant mobilization or demobilization.

Recent advancements in electrical geophysical characterization and monitoring techniques are being used at the Hanford Site to address each of these needs. Electrical imaging is useful because subsurface electrical properties (e.g. electrical conductivity) are directly influenced by the parameters that govern flow and transport in the vadose zone including grain size distribution, packing, and saturation [1,2]. Electrical properties are also sensitive to geochemical parameters altered by contaminants, amendments, and remedial processes. These include pore water geochemistry, mineralogy, and pore-grain interfacial electrochemistry [3,4,5]. Therefore, changes in electrical properties estimated via 3D geophysical imaging are proxies for corresponding changes in relevant remedial properties (e.g. changes in pore geochemistry, pore-grain interface alterations, changes in saturation, etc). Pre-remediation images of electrical properties provide baseline information concerning contaminant distribution and reduce uncertainty concerning the distribution of parameters that govern flow and transport. Time-lapse imaging can be used to monitor amendment transport and delivery, and to monitor post-delivery remedial performance using changes in electrical properties as proxies for changes in geochemical properties. Furthermore, 3D electrical geophysical monitoring hardware is commercially available, relatively robust, inexpensive, and can be operated autonomously.

Contemporary ERT data collection hardware allows autonomous collection of large amounts of data over short periods of time, providing the potential to characterize and monitor subsurface processes at unprecedented spatial and temporal resolution. Realizing this potential requires 1) high performance computing systems and parallel ERT modeling and inversion codes capable of efficiently processing large data sets and 2) an understanding of the relationship between temporal and spatial changes in hydrologic, geochemical and corresponding electrical properties. In this paper, we demonstrate high performance ERT imaging for both characterization and monitoring within the Hanford BC-Cribs and Trenches (BCCT) waste disposal area, where contaminated waste water was discharged into soil infiltration galleries (cribs and trenches) and drove contaminants deep into the vadose zone. Currently those contaminants continue to migrate toward the groundwater with the disposed water and subsequent natural recharge. We first demonstrate high performance ERT characterization of contaminant distribution using a large scale reconnaissance surface ERT survey collected over the BC-Cribs and Trenches area from 2004 to 2006. We then demonstrate a focused time-lapse ERT monitoring application during a desiccation treatability test conducted from January to July 2011. Soil desiccation is being evaluated as a remedial technology at the Hanford Site because removing pore water decreases the net forces driving contaminants to groundwater. This *in situ*

remediation technology has potential given the thick vadose zone and arid conditions found at Hanford. Time-lapse ERT monitoring executed during the desiccation treatability test demonstrated that ERT imaging provides high resolution 3D information concerning soil texture, contaminant distribution, gas flow distribution during desiccation, the progression of the desiccation zone, and post desiccation stability.

Reconnaissance ERT Characterization of the BCCT

ERT is a geophysical imaging method whereby the electrical conductivity of the subsurface is tomographically reconstructed using measurements of the subsurface electrical potential field generated during an induced current flow [6,7]. For a given measurement, current is injected between two electrodes, and the resulting potential between one or more sets of dislocated electrodes is observed. Many such measurements are strategically collected and processed to reproduce an approximation of the subsurface electrical conductivity giving rise to the measurements using a mathematical inversion algorithm. In conditions common to those found in the BCCT vadose zone, electrical current travels primarily through pore fluids such that bulk electrical conductivity is highly correlated to pore fluid conductivity [5]. Pore fluid conductivity is in turn governed by ionic strength or aqueous contaminant concentration, making electrical conductivity a useful metric for understanding subsurface contaminant distribution. The target contaminant for ERT is nitrate, which was released in large volumes at the BCCT, and is generally co-located with Tc-99 [8], a primary contaminant of concern due to its concentration and mobility in the vadose zone.

For the BCCT area characterization example [9], approximately 7500 electrodes were used to collect approximately 125000 ERT measurements in an effort to characterize zones of elevated electrical conductivity arising from high nitrate concentrations (Fig. 1). The spatial extent of the survey area, the number of electrodes, and the number of measurements in this data set presents a significant computational challenge to complete the inversion in a manner such that all of the information provided by the data is extracted and represented in the ERT image in terms of image resolution. To meet this challenge, the data are inverted on a parallel computing system leveraging a recently developed parallel ERT inversion code [10]. The inversion was executed on Hopper, a distributed memory supercomputer housed at the National Energy Research Scientific Computing Center. The inversion required approximately 6 hours of computing time using 800 processors, and estimated approximately 950,000 electrical conductivity values on an unstructured mesh using a regularized inversion technique [10].

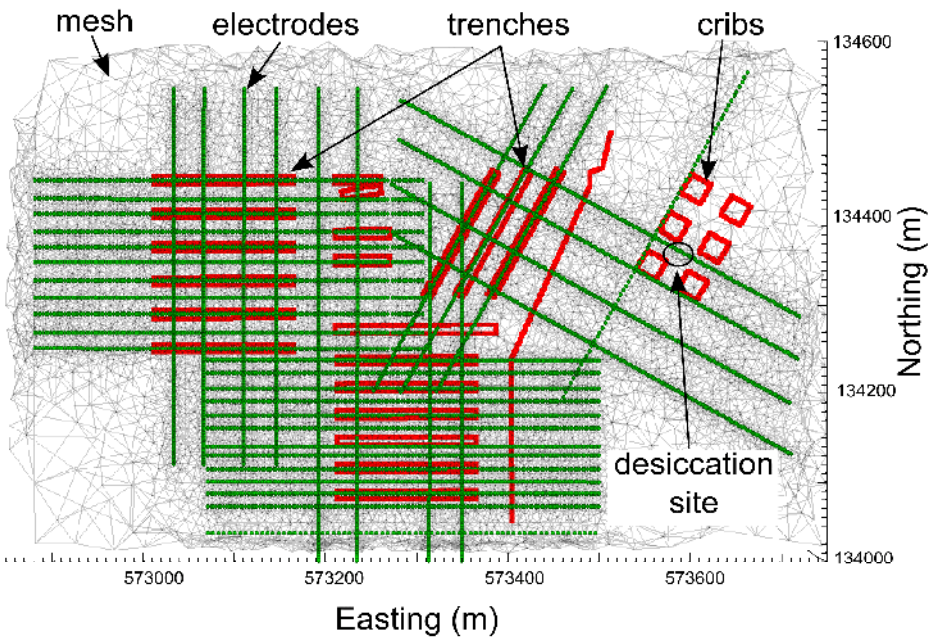

Fig. 1. ERT electrode line locations, computational mesh, and locations of cribs and trenches for a large scale ERT reconnaissance survey [9].

Results of the 3D characterization inversion are shown in figure 2. Figure 2-A,B and C show horizontal sections of the estimated subsurface electrical conductivity at depths of 20, 30, and 40 meters respectively. As shown in the color scale, the warmer colors represent elevated electrical conductivities associated with elevated saturation and/or elevated ionic strength. The ERT images suggest increased contaminant concentrations beneath the trenches, with several trenches displaying focused contamination consistent with disposal inventories. The highest conductivities are found beneath the cribs, which is consistent with the relatively high concentrations of contaminants discharged in the cribs area. Figure 2D shows an alternative representation of the ERT image. Here several isosurfaces of elevated electrical conductivity shown in an oblique view indicate the zones of highest contaminant concentration with respect to each infiltration gallery. These elevated zones are consistent with documented waste releases at the site. Overall, the ERT imaging suggests widespread contamination beneath the BCCT, but also locates several focused areas of elevated contamination that are not evident using inversions on coarser inversion grids required by a non-parallel inversion codes due to memory limitations.

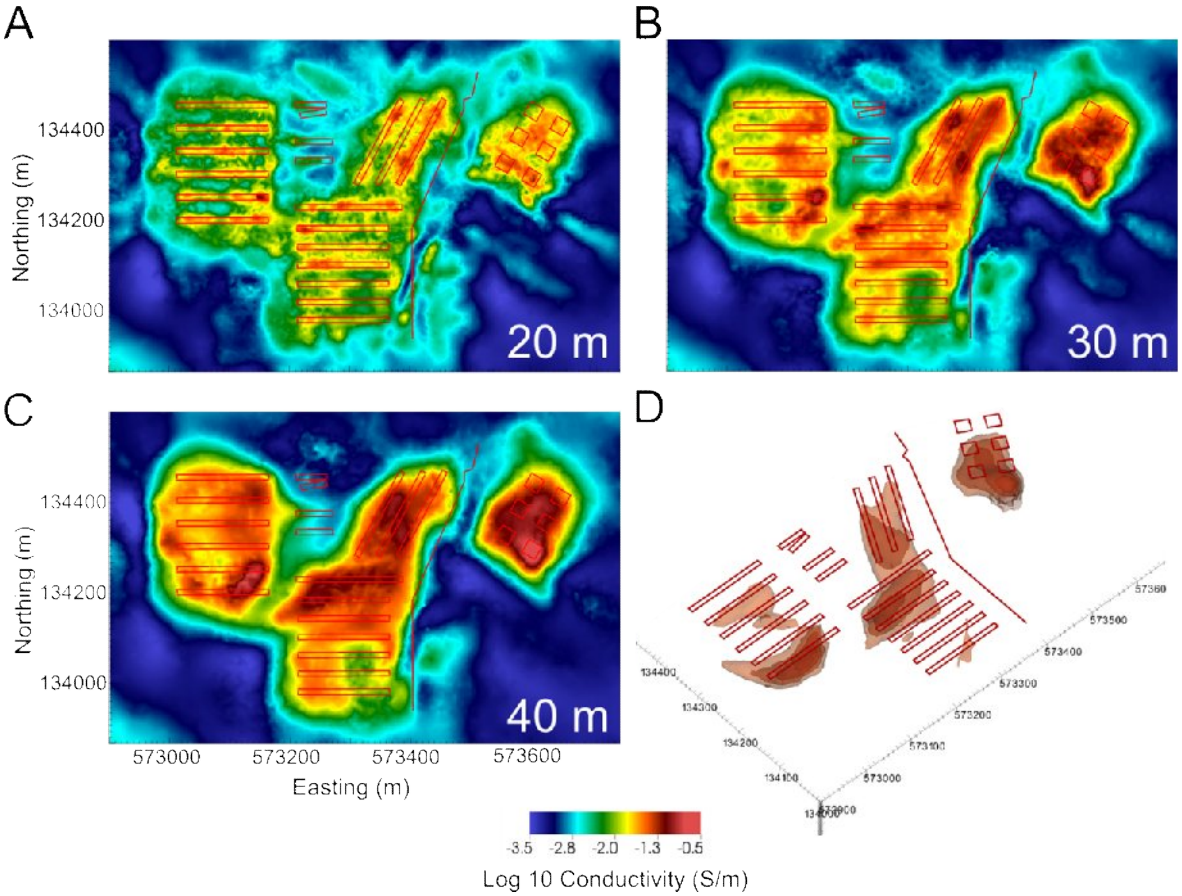

Fig. 2. Horizontal section of ERT inversion results at a depths of 20m (A), 30m (B), and 40 m (C). D) Oblique isosurfaces of elevated electrical conductivity with respect to cribs and trenches. Warmer colors represent elevated electrical conductivities associated primarily with elevated nitrate concentrations.

3D Time-lapse Imaging of the Desiccation Treatability Test

The desiccation treatability test was conducted in the cribs area at the location shown in figures 1 and 2. During the test, which ran from January through July 2011, dry nitrogen gas was injected over a depth interval of approximate 9 to 15 meters below ground surface, and extracted over the same depth interval at a well approximate 12 meters away. As dry nitrogen gas evaporates and transports pore water to the extraction well, a desiccation zone develops first around the injection well, and progressively migrating toward the extraction well with time. Note that electrical conductivity within the vadose zone displays a strong positive correlation with water content, enabling ERT to image the desiccation progress. With this in mind, a borehole electrode array consisting of 9 boreholes with 11 equally spaced vertical electrode strings was installed allowing baseline ERT characterization of the test site and time-lapse monitoring of desiccation progress.

Figure 3 shows the pre-desiccation subsurface electrical conductivity distribution. In this image, two electrical conductivity isosurfaces are superimposed on a transparency of the full solution to highlight the high and low values. The lens of elevated conductivity shown at the center of the image was verified by borehole logging to consist of a finer grained material of elevated water content and ionic concentration. Note that the desiccation site is not located directly beneath a crib, the nearest crib being several tens of meters to the northwest. The contaminant lens likely indicates of lateral migration of solution away from the cribs as driven by capillary forces.

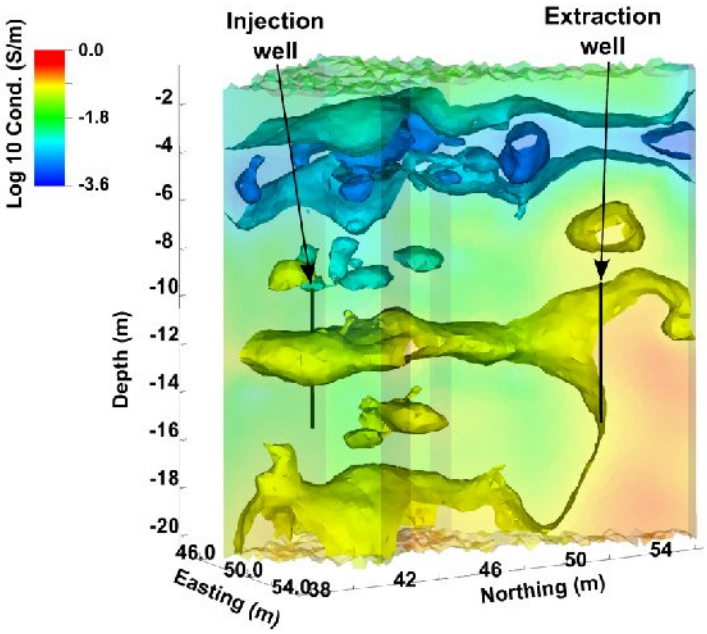

Fig. 3. Pre-desiccation 3D ERT isosurface image of electrical conductivity at the BCCT desiccation treatability site. Warmer colors indicate elevated conductivities associated with finer-grained, lower permeability materials of relatively high water content and contaminant concentration.

The expected behavior of the desiccation system can be informed from the pre-desiccation ERT image. For example, the elevated conductivity lens is diagnostic of finer-grained relatively low permeability materials, which may therefore impede and serve as a boundary for vertical gas flow. Lower conductivity units above and below the lens are diagnostic of coarser grained, higher permeability materials through which gas will preferentially flow. The prediction here would be that desiccation would first occur above and below the high conductivity lens as gas flows primarily above and below from the injection to the extraction well.

During the time-lapse monitoring phase of the desiccation test, ERT surveys are collected and inverted on a continuous cycle. Time lapse data are inverted in a manner similar to the pre-desiccation inversion. Once each time-lapse ERT image is produced, the pre-desiccation image is subtracted to reveal only the regions where electrical conductivity has changed with time.

Decreases in electrical conductivity are diagnostic of decreases in water content, and indicate where desiccation is occurring. ERT surveys were collected twice per day over the course of the desiccation experiment. Figure 4 shows monthly images of changes in conductivity from baseline and suggests that the primary zone of desiccation advances from the injection to the extraction well and occurs directly beneath the elevated conductivity lens revealed in the pre-desiccation characterization image (fig. 3).

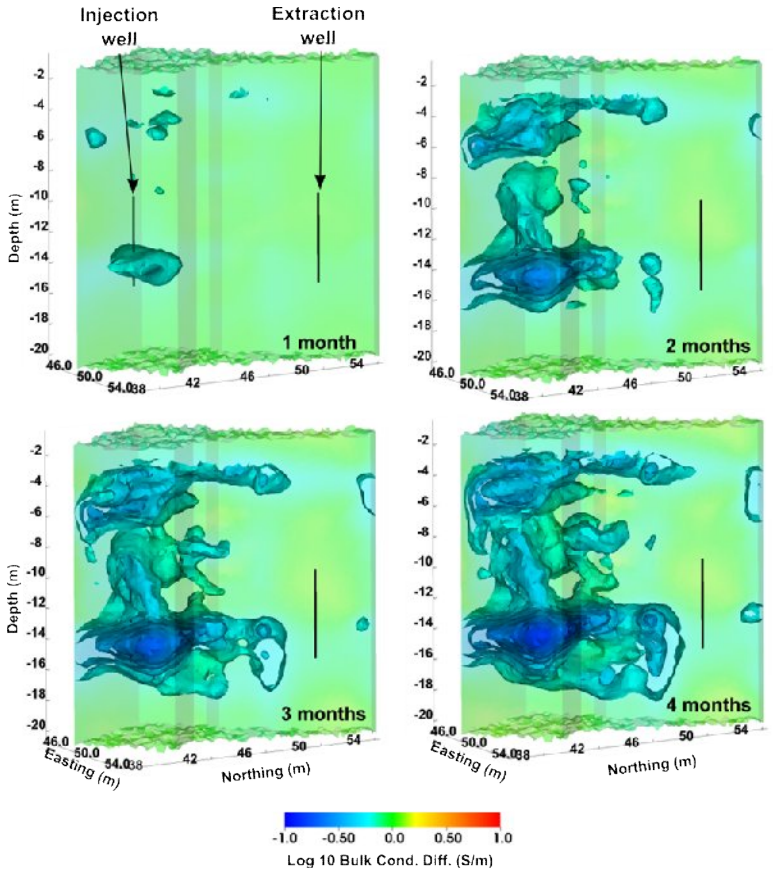

Fig. 4. Monthly 3D ERT images of changes in electrical conductivity cause by decreasing water content during the desiccation treatability test. The primary zone of desiccation occurs between 14 m and 16 m depth, directly below the high conductivity (low permeability) lens revealed in the pre-desiccation ERT image.

DISCUSSION

Two examples of ERT imaging at a former waste disposal facility have been demonstrated at different scales; a large scale reconnaissance survey spanning many hundreds of meters and a detailed monitoring application spanning a few tens of meters. Although ERT is applicable at many scales, resolution is generally governed by proximity to electrodes. For instance, the BCCT reconnaissance survey demonstrated herein lost resolution with depth (i.e. away from surface electrodes), and was unable to detect a high conductivity anomaly at approximately 75

m below ground surface in the cribs area; the deep anomalies were detected during highly focused borehole sampling. Conversely, the desiccation site characterization and monitoring demonstrated high resolution at a small scale, but only because of close proximity to survey electrodes. Although proximity to electrodes is not the only factor governing ERT resolution, it is often the primary factor for determining how an ERT system should be effectively deployed for a given application.

Regardless of resolution limitations, the utility of ERT for remotely detecting wastes and monitoring subsurface processes is evident. ERT imaging is not a final detection or monitoring solution alone, but provides a necessary capability to remotely detect subsurface conditions and understand subsurface processes. Such a capability can significantly increase the efficacy and reduce the cost of remediation by guiding sampling efforts and informing remedial system design and operation. However, given the computational demands of 3D ERT characterization and monitoring inversions, the full imaging capability enabled by contemporary ERT survey systems can generally only be realized with high performance computing resources, both hardware and software.

REFERENCES

[1] Lesmes, D.P. & Morgan, F.D., 2001. Dielectric spectroscopy of sedimentary rocks, *J. geophys. Res.,* **106**(B7), 13 329–13 346.

[2] Krumbein,W.C. & Monk, G.D., 1942. Permeability as a function of the size parameters of unconsolidated sand, *Am. Inst. Met. Engr.*, Tech. Publ.

[3] Leroy, P. & Revil, A., 2004. A triple layer model of the surface electrochemical properties of clay minerals, *J. Colloid Interface Sci.,* **270**(2), 371–380.

[4] Leroy, P. & Revil, A., 2009. A mechanistic model for the spectral induced polarization of clay material, *J. geophys. Res.,* **114,** B10202, doi:10.1029/2008JB006114.

[5] Archie, G.E., 1942, “The electrical resistivity log as an aid in determining some reservoir characteristics,” Transactions of the American Institute of Mining and Metallurgical Engineers, Vol. 146, pp. 54-62.

[6] Sasaki, Y., 1994, 3-D resistivity inversion using the finite-element method: Geophysics, **59**, 1839–1848.

[7] Günther, T., C. Rücker, and K. Spitzer, 2006, Three-dimensional modeling and inversion of DC resistivity data incorporating topography—II. Inversion:Geophysical Journal International, **166**, 506–517.

[8] Ward, A.L., G.W. Gee, Z.F. Zhang, and J.M. Keller, 2004. Vadose Zone Contaminant Fate-and-Transport Analysis for the 216-B-26 Trench, PNNL-14907, Pacific Northwest National Laboratory, Richland, WA.

[9] Rucker, D.F., M.T. Levitt, and W.J. Greenwood, 2009. Three-dimensional electrical resistivity model of a nuclear waste disposal site. Journal of Applied Geophysics 69:150-164.

[10] Johnson, T.C., R.J. Versteeg, A. Ward, F.D. Day-Lewis, and A. Revil, 2010. Improved hydrogeophysical characterization and monitoring through parallel modeling and inversion of time-domain resistivity and
induced-polarization data. Geophysics, 75(**4**), WA27-WA41.